Research Article – Vol. 02, Issue 04, No. 02

Advanced in Engineering and Intelligence Systems

Journal Web Page: https://aeis.bilijipub.com

Numerical investigation of motive pressure on condensation and evaporation process in steam ejector of renewable refrigeration system

RAKIBUL ISLAM[1, *], Amır Sohel[1], Md Faısal Bın Ashab[1]

[1] *College of Electrical Engineering and new energy, Three Gorges University, China*

Highlights

- Emphasis on finding low-energy consumption cycles for cooling processes, particularly relevant in regions with high temperatures and significant electrical energy consumption in air-conditioning and refrigeration industries.
- Recognition of the ejector refrigeration cycle as a suitable option due to its low energy consumption and environmental compatibility.
- Utilization of the k-wSST turbulence model and non-equilibrium condensation model to effectively simulate the ejector, showcasing a comprehensive approach to studying its performance.
- Investigation into the impact of motive flow pressure on various aspects of the ejector's performance, including temperature, Mach number, entropy production, and Coefficient of Performance (COP).
- Detailed analysis of flow behavior in the ejector, considering factors such as oblique shocks and shock train, and the significant influence of motive flow pressure on the entrainment ratio, a key parameter in ejector performance.

Article Info

Received: 17 August 2023
Received in revised: 21 October 2023
Accepted: 30 December 2023
Available online: 31 December 2023

Keywords

Ejector refrigeration cycles,
Steam ejector,
Entrainment ratio,
Entropy generation,
COP

Abstract

In today's life, it is very necessary to use cooling systems in the domestic and industrial cooling process, and the air-conditioning and refrigeration industry has the highest rate of electrical energy consumption in countries with hot weather. Therefore, it is very important to find a cycle with low energy consumption. Ejector refrigeration cycle can be a suitable option due to low energy consumption and compatibility with the environment. This study investigates the effect of pressure of motive flow on refrigeration cycle's ejector performance. The k-wSST turbulence model and the non-equilibrium condensation model are used to simulate the ejector. According to the results, the present model can well predict the flow behavior in the ejector. As the pressure of motive flow increases, the minimum pressure and minimum temperature in the ejector decreases and the maximum Mach number increases in the ejector, and the production entropy and COP decrease. The pressure of motive flow has a significant effect on the oblique shocks and shock train. The entrainment ratio, which is one of the most important parameters of the ejector, decreases with increasing pressure of motive flow. As the pressure increases from 1.98 bar to 4.75 bar, the entrainment ratio decreases by 62%, the primary flow rate increases from 0.000693 kg/s to 0.001597 kg/s, and a 130% increase in the primary flow rate is seen.

Nomenclature

E	*Total energy (J)*	***Greek symbols***	
ER	*Entrainment ratio*	γ	*Heat capacity ratio*

* Corresponding Author: RAKIBUL ISLAM
Email: rrakibulislam0123@gmail.com

h	*Enthalpy* (J/kg)	ρ	*Density* (kg/m^3)
J	*Nucleation rate* $(1/kg.s)$	μ	*Dynamic viscosity* $(Pa.s)$
Kn	*Knudsen number*	λ	*Thermal conductivity* $(W/m.K)$
$\dot{m}$	*Mass flow rate* (kg/s)	τ	*Viscous stress tensor* (Pa)
n	*Droplets number* $(1/kg)$	θ	*Non-isothermal*
P	*Pressure* (Pa)	σ	*Surface tension* (n/m)
q_c	*Condensation coefficient*	Γ	*Mass source* $(kg/m^3.s)$
r	*Droplet radius* (m)	***Subscripts***	
T	*Temperature* (K)	d	*Discharge*
u, v	*Velocity components* (m/s)	$grow$	*Growth*
x	*Cartesian direction* (m)	l	*Liquid*
y	*Mass fraction of liquid*	lv	*Liquid-vapor*
Abbreviations		nuc	*Nucleation*
ER	*Entrainment ratio*	p	*Primary*
POMF	*Pressure of motive flow*	s	*Secondary*
LMF	*Liquid mass fraction*	v	*Vapor*
PN	*Primary nozzle*		
ERC	*Ejector refrigeration cycle*		

1. Introduction

The air-conditioning and refrigeration industry has the highest rate of electrical energy consumption in countries with warm climates. It is necessary to use the cooling systems used in the process of domestic cooling, industrial and air conditioning in today's modern life. On the other hand, conventional cooling systems that use vapor-compression cycle cause high consumption of electrical power [1-3]. The mechanical compressor consumes the most electricity in the system. This type of system leads to an increase in global electricity consumption. However, there are other types of refrigeration systems that mainly use thermal energy to run the system with a small amount of electricity. These types of thermal refrigeration systems are called. Renewable energies such as solar energy [4], geothermal energy [5] or even heat loss from the production process can be used as a heat source in these systems. Boiler, ejector and pump in the ERC have been replaced instead of the compressor in steam compression cycles [6-7]. Figure 1 shows an ERC.

Nowadays, ejector simulation using computational fluid dynamics has attracted the many researchers attention. Bartosiewicz et al. [8] used six well-known turbulence models in a supersonic air ejector in a numerical simulation and compared the results with the experimental results. According to the results, the k-wSST turbulence model had a further fit with the empirical points in the static pressure distribution in the center line of the ejector than other turbulence models. But k-e and RNG turbulence models performed better than other models in predicting the shock position. Hamidi et al [9] investigated the behavior of two turbulence models k-e and k-wSST in the ejector. According to the results, when the primary nozzle (PN) inlet pressure increases, the difference between these two models is very small. Riffat et al. [10] simulated the behavior of the flow in the ejector using computational fluid dynamics and showed that the efficiency of the ejector is dependent on the PN and its position. Varga et al. [11] examined the effect of geometrical parameters on the efficiency of the ejector numerically and investigated the changes in the suction rate compared to the condenser pressure in different area ratios. The area ratio refers to the ratio of the mixing chamber diameter to the diameter of the PN. If the diameter of the PN is fixed, this ratio has a direct relationship with the mixing chamber diameter. As the area ratio increases, the ER also increases, at the same time, the critical pressure of the ejector decreases.

Zhou et al. [12] tried to find the optimal position of the nozzle outlet and the convergence angle of the mixing chamber by numerical simulation. According to 210 test results, the optimal position of the nozzle outlet is not only proportional to the throat diameter, but this position increases with the increase of the initial flow pressure, and the efficiency of ejector is very sensitive to the angle of convergence, especially near the optimal working point. The suction ratio can change up to 26.6% by changing the convergence angle. Chen et al [13] studied the natural gas ejector to investigate the effects of geometrical factors to maximize the ER, and obtained the optimal geometrical factors. According to the numerical results, the mixing chamber optimal angle is 14 degrees, the ratio of the mixing tube optimal diameter to the initial nozzle pit is 1.7, the ratio of the length to the diameter of the optimal mixing tube is 5.0, and the diffuser optimal angle is 1.43 degrees. A field experiment was conducted in order to validate the numerical results. The ratios obtained from the numerical simulation were consistent with the field data. A consistency between the ratios obtained from the numerical solution and the field data was observed.

Lee et al. [14] studied gas-gas and condensing (gas–liquid ejector) ejectors. This study has concluded the changes in the ER in relation to the ratio of the length to the

diameter of the mixing chamber in the rate of different areas and different driving fluids. These changes were investigated respectively when the working fluid is nitrogen-nitrogen and nitrogen-water. The ER increased in both of them with the increase in the ratio of the length to the diameter of the mixing chamber, and then it decreased more noticeably in the case of nitrogen-water, but this ER also increased.

Chen et al. [15] investigated the supersonic ejector used in the oil and gas industry. Their main focus was on the two geometrical parameters of the PN exit position and the ratio of the length of the mixing chamber to its diameter (R). In their classification, the diameter of the mixing chamber is fixed, and there is a direct relationship between the increase and decrease of the R value with the length of the chamber. The changes of pressure rate and ER were investigated with respect to the R parameter at different pressures from the initial flow. As can be seen in the figure, both pressure rate and strain rate parameters first increase and then decrease with the increase of R, and in this way, an optimal value for the length of the chamber is obtained. Maghsoodi et al. [16] also examined the effect of length and angle of divergence in continuation of their geometric studies on ejector performance. The variation of the ER with respect to the diverging angle of the diffuser was investigated in different lengths of it. According to the results, firstly with the increase of the divergence angle, the ER also increases and then its value decreases, and an optimal value is obtained for the diffuser divergence angle where the ejector has the highest ER. Also, as the length of the diffuser increases, the value of the ER increases, and at the same time, the optimal divergence angle of the diffuser decreases. Chen et al. [17] also carried out their geometric studies on an ultrasonic air ejector in order to improve its performance. In their studies, they found an optimal value of the initial nozzle outlet position, so that the ejector had the highest ER.

Yang et al. [18] examined the effect of nozzle shape on the steam ejectors efficiency. They considered 5 nozzles and simulated them numerically. They concluded that the ER and pressure of critical in a rectangular nozzle are 7.1% and 21.3% less than a nozzle conical, in an elliptical nozzle it is 7.9% and 21.3% less than a conical nozzle, and in a square nozzle it is 2% and 2.1% less than a conical nozzle, but in the cross-shaped nozzle, the entrainment rate was 9.1% better than the conical nozzle and the critical pressure was 6.4% lower than the conical nozzle.

Condensation phenomenon [19-21] is one of the differences between numerical and laboratory works in the ejector, which often consider the fluid flowing in it as a dry gas for simplicity and reduction of simulation time [22]. But some researchers considered the fluid passing through the ejector as wet vapor in order to be more accurate and closer to reality [23]. Although this action is consistent with reality, it adds the equations of budding and growth of drops as a set of equations, which increases the volume and time of calculations [24].

Ariafar et al. [25] compared the entrainment rate and the critical end pressure for two states of wet steam and dry steam. According to the results, wet steam flow predicts a higher ER and critical end pressure. They calculated the mixing layer growth for wet vapor and dry vapor states. According to the result, the size of the mixing layer is larger for wet steam than for dry steam. In another study, Ariafar et al. [26] studied the impact of mixing layer and mixing pressure on ER. In the research conducted, the growth of the mixing layer was validated with laboratory results. Ariafar et al [27] examined the impact of the PN cross-sectional area ratio and the enlargement of the mixing layer in the steam ejector, and compared the results of the wet steam state with the dry steam state. They used the empirical results in the nozzle of Moore for validation. They considered three PN cross-sectional area ratios of 11, 18 and 25 to simulate their work.

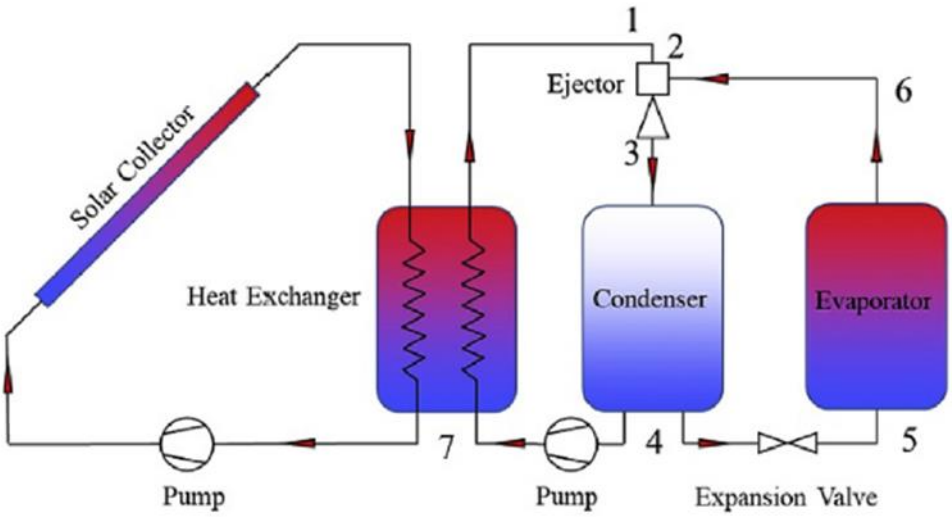

Fig 1. Ejector refrigeration cycle [23]

Nowadays, the use of the ERC that uses steam as a refrigerant is very important due to environmental issues. Any factors affecting the COP need to be investigated and studied due to the low COP of these cycles. This study considers a steam ERC, and examines the effect of POMF on the processes of condensation and evaporation, expansion and condensation of flow, flow behavior and ER. This study examines the effect of the POMF on the performance of the ERC and its effect on the COP and the behavior of the fluid inside the ejector.

2. Governing equations and solution details

The Navier-Stokes equations together with the equations of droplet number and wetness have been solved using the Eulerian-Eulerian viewpoint [28] and the method of single-fluid [29] in this study. This method considers the vapor and liquid phase as one phase and the equations are solved for the mixed phase, and the sliding speed between the vapor and liquid phases is ignored due to the small diameter of the water droplets [30]. The following assumptions are considered for the equations governing the ultrasonic ejector [23]:

- The effects of gravity on the steam inside the ejector are ignored.
- The flow has axial symmetry.
- The flow is solved in the steady frame.

The equations of continuity, momentum, energy, number of drops and humidity are as follows [31].

$$\frac{\partial \rho}{\partial t}+\frac{\partial(\rho u_j)}{\partial x_j}=0 \quad (1)$$

$$\frac{\partial(\rho u_i)}{\partial t}+\frac{\partial(\rho u_j u_i+P\delta_{ji})}{\partial x_j}-\frac{\partial \tau_{ji}}{\partial x_j}=0 \quad (2)$$

$$\frac{\partial(\rho E)}{\partial t}+\frac{\partial(\rho u_j H)}{\partial x_j}+\frac{\partial(q_j-u\tau_{ji})}{\partial x_j}=0 \quad (3)$$

$$\frac{\partial(\rho y)}{\partial t}+\frac{\partial(\rho u_j y)}{\partial x_j}=\Gamma_1+\Gamma_2 \quad (4)$$

$$\frac{\partial(\rho n)}{\partial t}+\frac{\partial(\rho u_j n)}{\partial x_j}=J \quad (5)$$

Where, P is pressure, ρ is density, y is humidity, and h is enthalpy. The subscripts v and l refer to the vapor and liquid phases, respectively. The classical nucleation equation is given by [32].

$$J_{class}=q_c\sqrt{\frac{2\sigma_r}{\pi}}m_m^{-3/2}\frac{\rho_v}{\rho_l}exp\left(\frac{-4\pi r^{*2}\sigma_r}{3K_bT_v}\right) \quad (6)$$

Corrections of Kantrowitz is utilized in the equation (6).

$$J=\frac{1}{1+\emptyset}J_{class} \quad (7)$$

$\emptyset$ is the temperature correction coefficient (8) [33].

$$\emptyset=2\frac{(\gamma-1)}{(\gamma+1)}\frac{h_{lv}}{RT_v}\left(\frac{h_{lv}}{RT_v}-\frac{1}{2}\right) \quad (8)$$

$\frac{dr}{dt}$ is the droplet growth [31].

$$\frac{dr}{dt}=\frac{1}{\rho_l}\frac{\lambda_v}{(1+3.18Kn)}\frac{r-r^*}{r^2}\frac{T_s-T_v}{h_v-h_l} \quad (9)$$

Two mass sources defined for phase change [34].

$$\Gamma_1=\frac{4}{3}\pi\rho_l\rho r^{*3}J \quad (10)$$

$$\Gamma_2=4\pi\rho_l\rho n r^2\frac{dr}{dt} \quad (11)$$

Two mass sources are used to define phase change for nucleation (Γ_1) and droplet growth (Γ_2). The major

parameter for an ejector can be described as entertainment ratio [35]. This parameter is defined as:

$$ER = \frac{\dot{m}_s}{\dot{m}_p} \quad (12)$$

where mass flow rates of primary and the secondary are depicted by $\dot{m}_p$ and $\dot{m}_s$, respectively. In solar-driven ejector refrigeration system, COP is equal to ER [36].

$$COP = \frac{h_s - h_D}{h_P - h_D} \quad (13)$$

The k-ω SST turbulence model has been used for the turbulence flow in the ejector [37]. The Roe's model is used to calculate the fluxes of convective. The governing equations discretization is performed with the upwind scheme and second-order accuracy. In the order of less than 10^{-8}

, the simulations are converged with root mean square residuals.

3. Results

The POMF is one of the significant parameters in the analysis of steam ejector behavior. The driving flow from the generator enters the PN of steam ejector, and the required vacuum in the evaporator is provided by the ejector. In this study, the primary flow and the secondary flow are in saturation, and the discharge pressure is 3.2 kPa and the secondary flow pressure is 1.28 kPa.

3.1. Validation and the independence of the solution from the computing grid

Two important issues in numerical solution are evaluated in this part. Validation shows the numerical solution accuracy. In validation, the experimental data are compared with the results obtained from calculations. In examining the independence of the solution from the computational grid, the effect of the number of grids on the numerical solution results is evaluated. In this part, the Ruangtrakoon ejector [38] is used to examine the two mentioned issues. The POMF, secondary flow pressure, and discharge pressure are 270 kPa, 1.08 kPa, and 3.5 kPa, respectively. Figure 2 shows the independence of the solution from the computing network. Three computational grids with the number of 15,000 cells, 32,000 cells, and 65,000 cells were considered, and the ER value was calculated. By increasing the number of computational cells from 32,000 to 65,000, the ER changes by about 0.1%, which is almost negligible. 32000 computing cells are used in this research due to the reduction of computing cost. Figure 3 shows the computational domain.

The numerical solution validation in the Ruangtrakoon ejector is shown in Table 1. The experimental value of the ER in the ejector is 0.44. The current numerical solution predicts the ER of 0.4315, and by comparing these two values, an error of 1.9% is reported. Table 1 shows that the considered numerical method is appropriate.

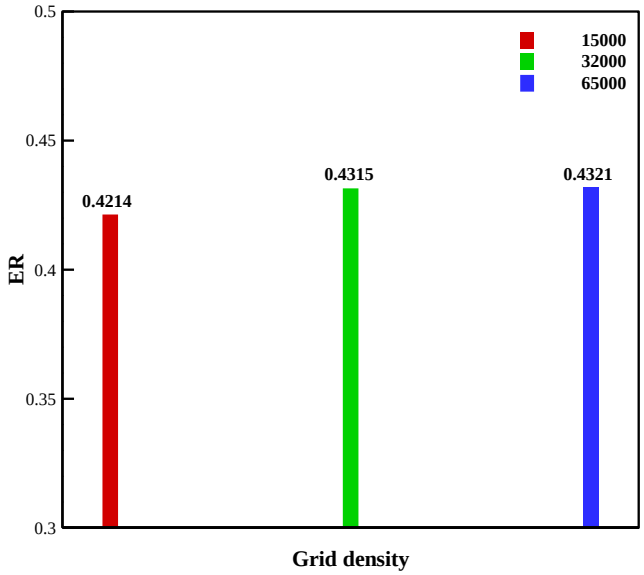

Fig 2. independence of the solution from the computing grid

Figure 3. Computation domain inside the ejector

Table 1. Validation of Ruangtrakoon ejector [38]. Primary, secondary and discharge pressures are 270 kPa, 1.037 kPa and 2.8 kPa.

	Experiment	Numerical	Error [%]
ER	0.44	0.4315	1.9

3.2. The impact of POMF on steam flow inside the ejector

The effect of the pressure driving flow on fluid flow behavior in the ejector is investigated in this section. Pressure, temperature and Mach number graphs are needed to check fluid behavior. Figures 4-6 show the distribution of pressure, temperature and Mach number inside the ejector, respectively. The pressures considered for the driving flow are: 232 bar, 312.9 bar and 415.3 bar. The driving flow in the PN reaches the supersonic state and creates a low-pressure zone at the end of the PN.

This low-pressure area is located approximately at 0.06 m<x<0.08 m. The temperature reaches the lowest value and the Mach number reaches the highest value in this region. The minimum pressure in the ejector is 130.5 Pa, 81.7 Pa, and 57.1 Pa for driving pressures of 232 bar, 312.9 bar, and 415.3 bar, respectively. Then, the pressure value reaches 1452 Pa, 1726 Pa and 1868 Pa respectively with the occurrence of shock. The minimum temperature for the driving pressures of 232 bar, 312.9 bar, and 415.3 bar is 172 K, 154 K, and 142 K, respectively, and when the shock occurs, the temperature reaches 323 K, 353 K, and 372 K. The maximum Mach number for the mentioned driving pressures are: 4.3, 4.75 and 5.12 and the Mach number reaches 2.63, 2.49 and 2.44 with the occurrence of shock d. After the low-pressure area, the pressure and temperature increase due to the occurrence of diagonal shocks and shock train, and the Mach number decreases. As the driving pressure increases, the intensity of oblique shocks increases.

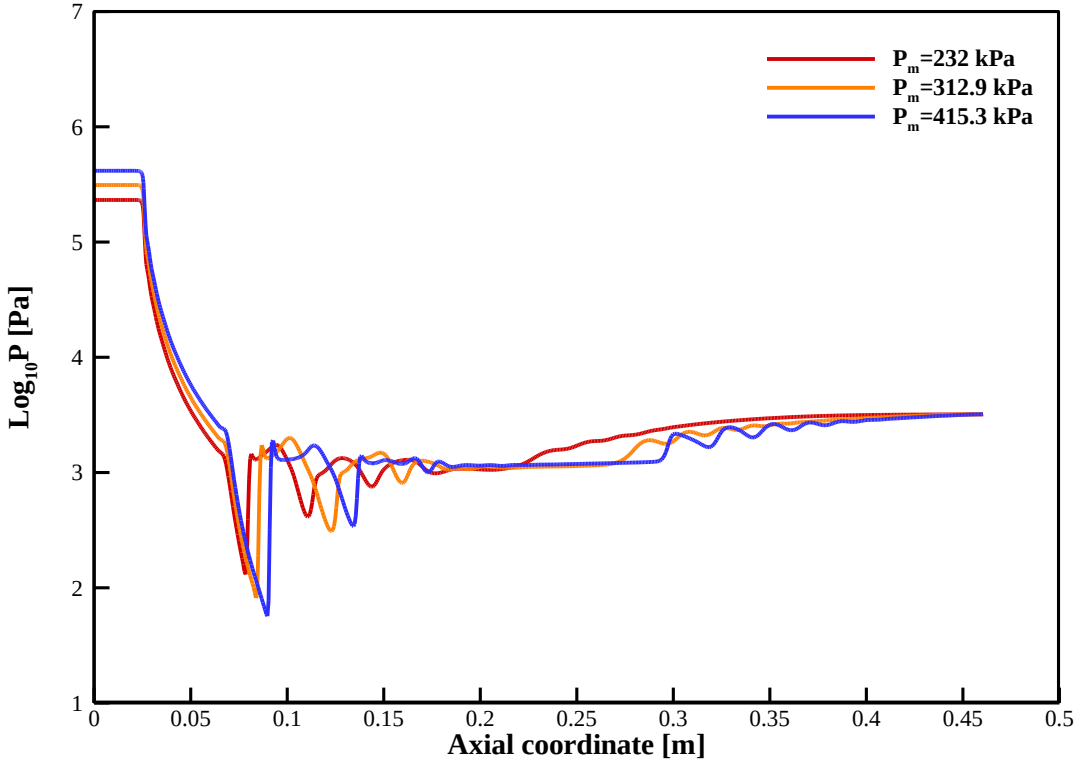

Figure 4. Impact of POMF on the pressure

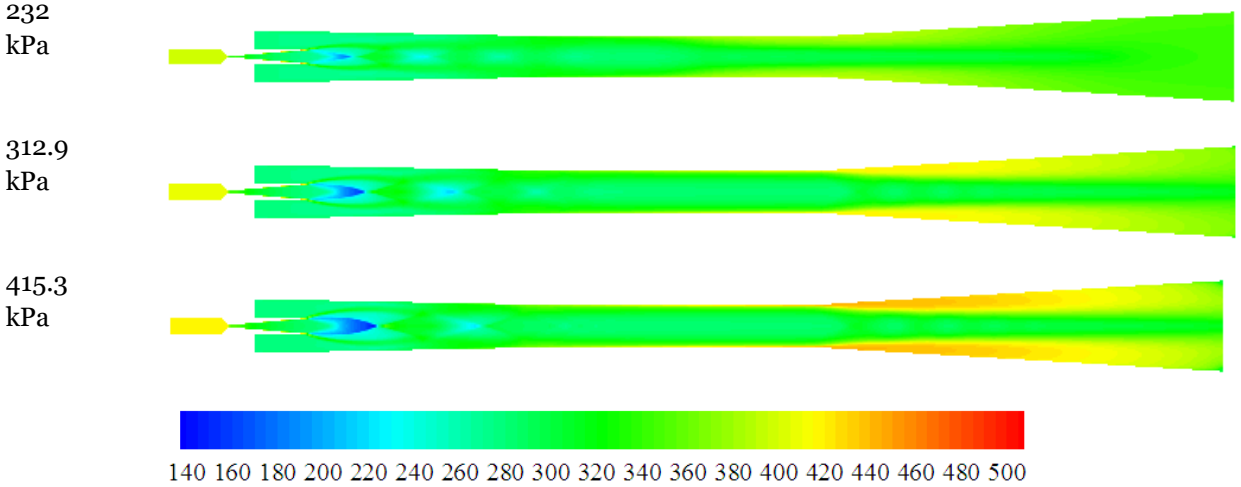

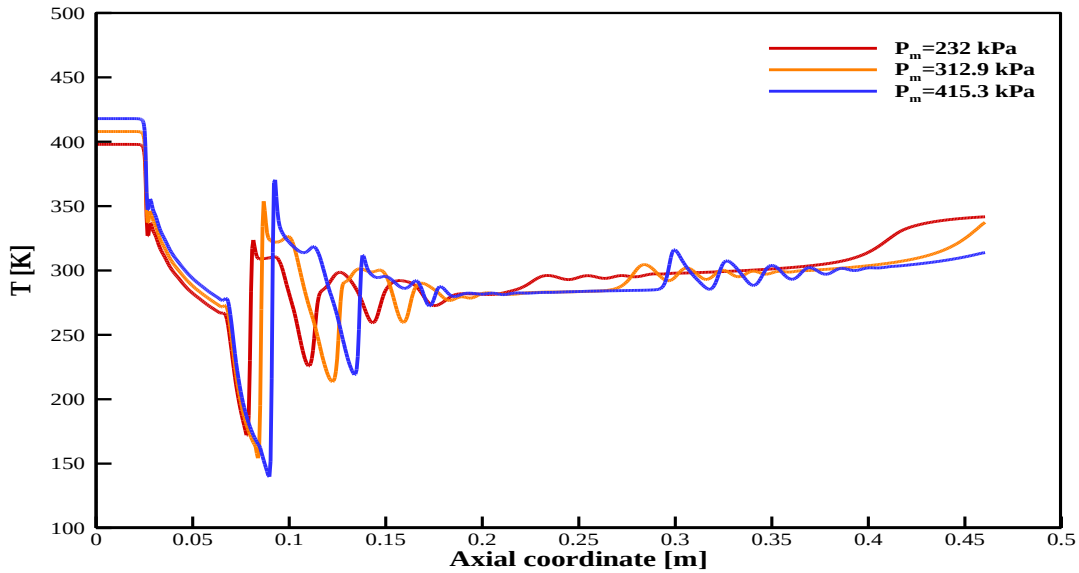

Figure 5. Effect of POMF on the temperature

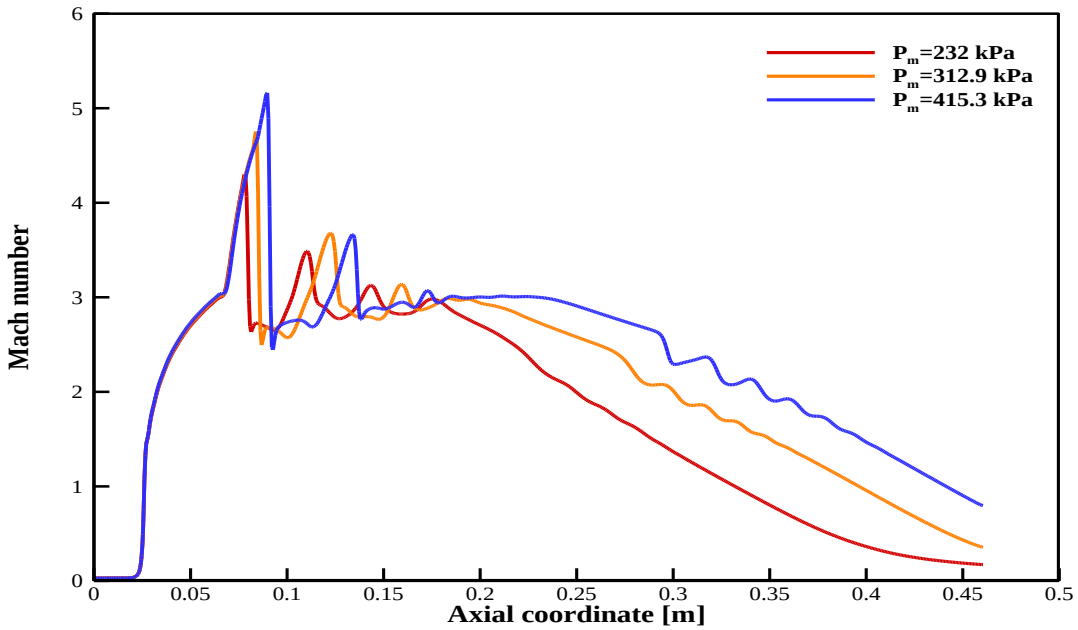

Figure 6. Effect of POMF on the Mach number

3.3. The impact of the POMF on the two-phase flow inside the ejector

Due to the occurrence of nucleation process in the PN of the steam ejector, very fine water droplets are formed spontaneously, and two-phase flow is seen in the ejector with the occurrence of condensation. The rate of nucleation in the central line of the steam ejector can be seen in Figure 7. Liquid droplets grow due to the condensation of vapor on their surface and their size decreases due to evaporation. The occurrence of oblique shocks and shock train affects the process of evaporation and condensation. Figure 8 indicates the distribution of the liquid phase in the ejector. The rate of nucleation happens at approximately x=0.023 m, and the liquid phase in Figure 8 is formed approximately at x=0.023 m, and its value increases rapidly. With the rapid expansion of the flow, the liquid phase increases, and reaches a maximum at approximately x=0.085 m.

As the POMF enhances the maximum liquid mass fraction (LMF) in the steam ejector increases. The maximum value of LMF for driving pressures of 232 bar, 312.9 bar and 415.3 bar is 0.234, 0.246 and 0.26, respectively. Then, the LMF in the ejector decreases with the occurrence of diagonal shocks and shock train. At a pressure of 232 bar for the driving flow, the LMF at x=0.41 m becomes zero. The LMF at the end of the ejector for pressures of 312.9 bar and 415.3 bar is 0 and 0.07, respectively. Figure 8 shows that the driving flow pressure has a great effect on the process of vapor condensation and liquid evaporation.

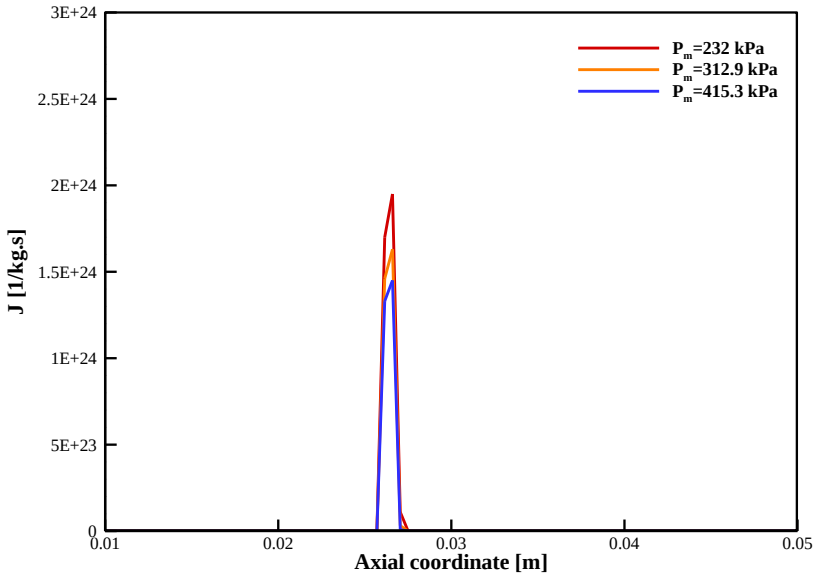

Figure 7. Impact of POMF on the nucleation rate

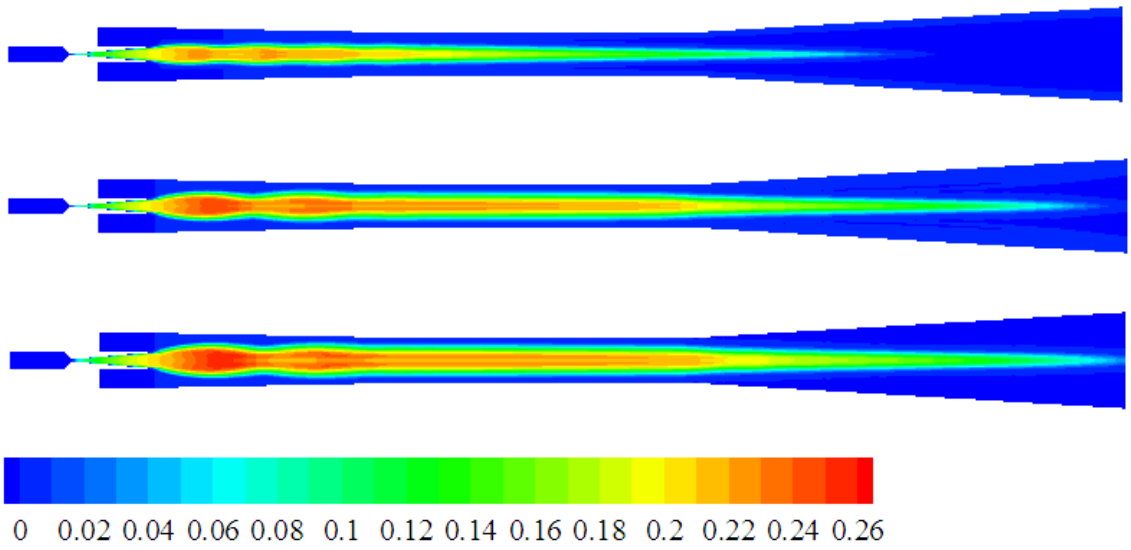

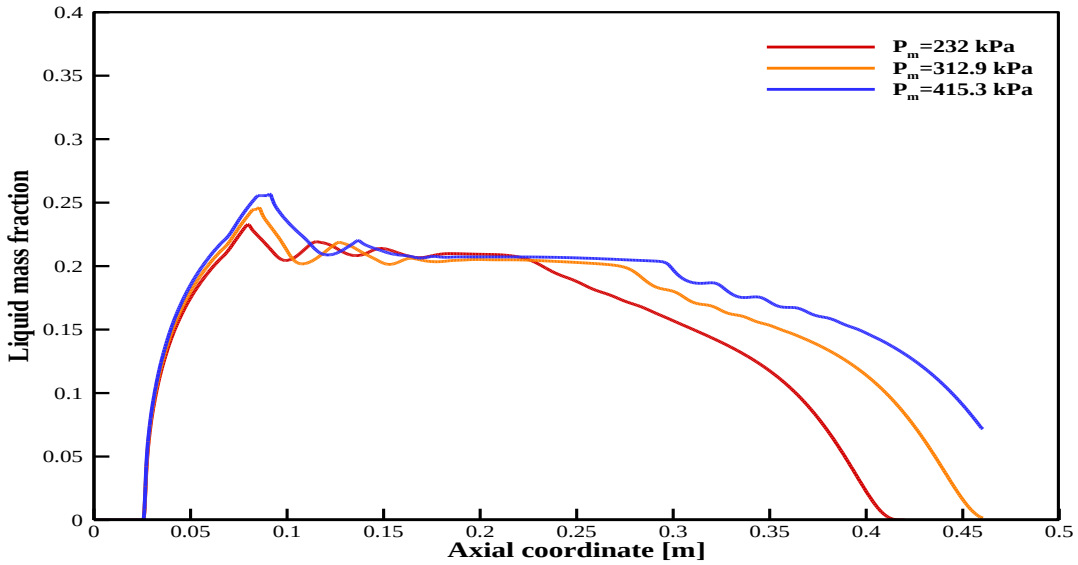

Figure 8. Effect of POMF on the LMF

3.4. The effect of the POMF on ER

The ER is one of the main parameters of an ejector, which represents the mass of the suction flow to the mass of the drive flow. Higher values of this parameter are more desirable. The effect of POMF on the ER, secondary flow rate and primary flow rate is indicated in Figure 9. As the POMF increases from 1.98 bar to 4.75 bar, the initial flow rate increases from 0.000693 kg/s to 0.001597 kg/s, and a 130% increase in the initial flow rate is seen. In other words, it can be said that an ascending trend can be seen in the initial flow rate. But the secondary flow rate is different. At the driving pressure of 1.98 bar, the secondary flow rate is 0.000496 kg/s, and by increasing the driving pressure to 2.32 bar, the secondary flow rate increases and reaches the value of 0.000535 kg/s.

Then, the mass flow rate of secondary flow decreases by increasing the driving pressure up to 4.75 bar. It can be said that an ascending-descending trend can be seen in the flow rate of the secondary flow with increasing pressure of the driving flow. The ER depends on the two parameters of primary flow rate and secondary flow rate. According to Figure 9, with the enhancement in the pressure of the driving flow, the ER decreases. As the pressure increases from 1.98 bar to 4.75 bar, the ER decreases by 62%. This shows that the driving pressure is a very important parameter in the ejector performance.

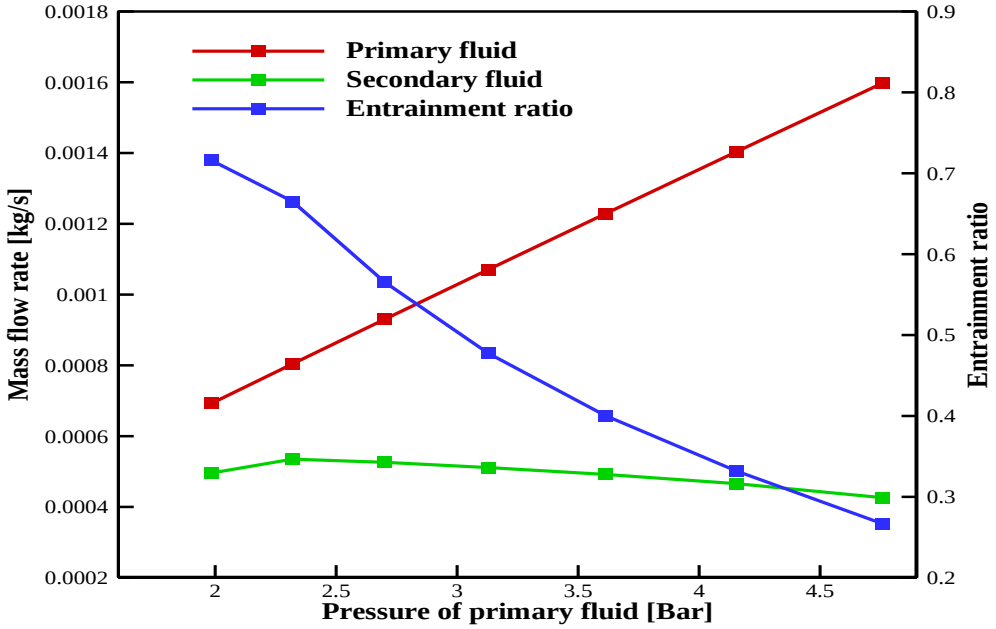

Figure 9. Effect of POMF on the ER, primary and secondary mass flow rates

3.5. The impact of driving flow pressure on production entropy

The impact of driving flow pressure on production entropy is investigated in this section. To compute the production entropy, the thermodynamics second law is applied. The production entropy for an adiabatic ejector is equal to:

$$S_{gen} = m_{out}s_{out} - m_m s_m - m_s s_s \quad (14)$$

The effect of the POMF on the production entropy is shown in Figure 10. As the driving flow pressure increases, the production entropy increases. By increasing the driving flow pressure from 1.98 bar to 4.75 bar, the production entropy increases from 1.11 W/K to 3.24 W/K, and an increase of 189% is observed. The POMF has a significant effect on the production entropy. Among the entropy production factors in the ejector, shocks, phase change, friction and flow mixing can be mentioned. According to Figures 4-6, the intensity of the shocks increased with the increase in the driving flow pressure, which increases the entropy production.

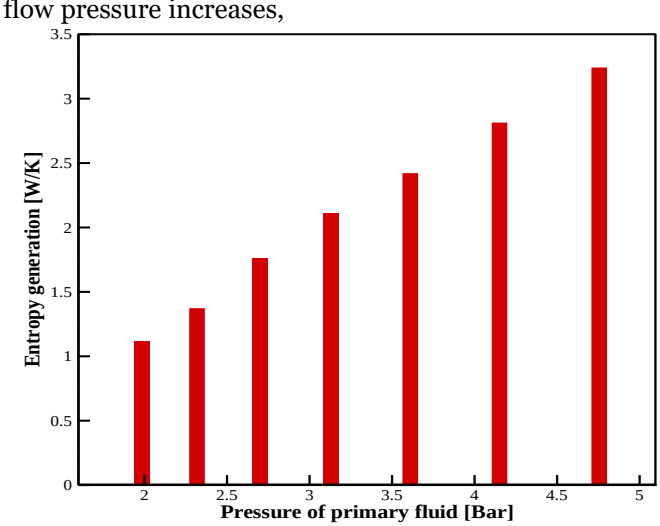

Figure 10. Effect of POMF on the entropy generation

3.6. The impact of motive flow pressure on COP

Figure 1 shows the schematic view of the ERC. The water heated by the solar collector is transferred to the generator, where the refrigerant of the ejector cycle evaporates. In the generator, the refrigerant reaches the required temperature and pressure, and enters the ejector. A low-pressure zone is created in the ejector which causes the flow to be sucked from the operator. Then, the flow entered from the generator and the flow sucked from the evaporator are combined and exited from the ejector outlet and transferred to the condenser. COP is one of the most important parameters of the refrigeration cycle, and the impact of the POMF on the COP of a refrigeration cycle is investigated in this section. The effect of driving pressure on COP is shown in Figure 11. COP decreases with the increase of driving flow pressure. As the driving flow pressure increases from 1.98 bar to 4.75 bar, the COP increases from 1.11 to 3.24, and a 60% decrease is observed. The reason for COP reduction can be predicted in the performance of the ejector. A decrease in the ER was seen with increasing pressure of the driving flow, and this indicates a decrease in the efficiency of the ejector. In fact, it can be said that the efficiency of the ERC depends on the ejector and the ejector is its most important component, and any improvement in the efficiency of the ejector will improve the cycle efficiency.

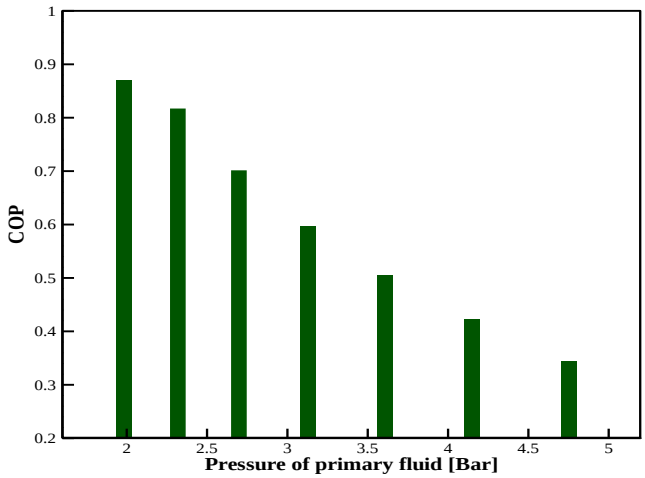

Figure 11. Effect of POMF on the COP

4. Conclusion

Nowadays, it is very important to use equipment that has the least environmental pollution. The ejector is one of the equipment that does not have any pollution. This study examines the impact of initial flow inlet pressure on behavior of flow, condensation and evaporation processes. First, the steam flow in the ejector is simulated, and the independence of the solution from the grid and validation are performed. Then, the impact of the initial flow inlet pressure is checked by considering the changes of the initial flow inlet pressure from 1.89 bar to 5 bar. The most important results are:

- A low-pressure zone is created in the ejector after the primary nozzle. As the pressure of the driving flow increases, the pressure and temperature of the low-pressure area decreases and the Mach number of this area increases.
- Diagonal shocks and shock train are seen in the ejector due to the rapid occurrence of compression-expansion processes. The intensity of the shocks increases with the increase of the driving pressure flow.
- The liquid-vapor phases are seen after the nucleation phenomenon occurs, and evaporation-condensation processes are seen in the flow. As the driving flow pressure enhances, the liquid phase produced in the ejector increases and the liquid mass fraction at the ejector outlet increases.
- An increase in the pressure of motive flow does not lead to an enhancement in the flow rate of the secondary flow and an ascending-descending trend is seen in the flow rate of the secondary flow, which causes the increase in the pressure flow of the driving flow to have a negative effect on the performance of the ejector and the entrainment ratio decreases. As the pressure increases from 1.98 bar to 4.75 bar, the entrainment ratio decreases by 62%.
- Occurrence of shocks, flow expansion and compression, friction, flow mixing and phase change cause entropy production. As the pressure of the driving flow increases, the entropy generated in the ejector increases.
- COP is one of the most important parameters of a refrigeration cycle, whose value decreased with the increase of driving pressure.

According to the results of this study, the pressure of motive flow has a significant effect on the efficiency of an ejector refrigeration cycle and its effect should be considered in the design, because any change in it causes a change in the ejector and cycle efficiency.

REFERENCES

[1] Kadam ST, Kyriakides AS, Khan MS, Shehabi M, Papadopoulos AI, Hassan I, Rahman MA, Seferlis P. Thermo-economic and environmental assessment of hybrid vapor compression-absorption refrigeration systems for district cooling. Energy. 2022 Mar 15;243:122991.

[2] Yıldız G, Gürel AE, Ceylan İ, Ergün A, Karaağaç MO, Ağbulut Ü. Thermodynamic analyses of a novel hybrid photovoltaic-thermal (PV/T) module assisted vapor compression refrigeration system. Journal of Building Engineering. 2023 Apr 1;64:105621.

[3] Jiang H, Rong Y, Zhou X, Fang S, Wang K, Zhi X, Qiu L. Performance assessment of an organic Rankine–Vapor compression cycle (ORC-VCR) for Low-Grade compression heat recovery. Energy Conversion and Management. 2023 Jan 1;275:116492.

[4] Sherwani AF. Analysis of solar energy driven organic

Rankine cycle-vapor compression refrigeration system. Thermal Science and Engineering Progress. 2022 Oct 1;35:101477.
[5] Li T, Li X, Gao H, Gao X, Meng N. Thermodynamic Performance of Geothermal Energy Cascade Utilization for Combined Heating and Power Based on Organic Rankine Cycle and Vapor Compression Cycle. Energies. 2022 Oct 4;15(19):7294.
[6] Direk M, İşkan Ü, Tunçkal C, Mert MS, Yüksel F. An experimental investigation of ejector employed a dual-evaporator vapor compression refrigeration system under various entrainment ratios using R134a as the refrigerant. Sustainable Energy Technologies and Assessments. 2022 Aug 1;52:102293.
[7] Baniasad Askari I, Ghazizade-Ahsaee H, Kasaeian A. Investigation of an ejector-cascaded vapor compression–absorption refrigeration cycle powered by linear fresnel and organic rankine cycle. Environment, Development and Sustainability. 2022 Jun 2:1-46.
[8] Bartosiewicz Y, Aidoun Z, Desevaux P, Mercadier Y. Numerical and experimental investigations on supersonic ejectors. International Journal of Heat and Fluid Flow. 2005 Feb 1;26(1):56-70.
[9] Hemidi A, Henry F, Leclaire S, Seynhaeve JM, Bartosiewicz Y. CFD analysis of a supersonic air ejector. Part I: Experimental validation of single-phase and two-phase operation. Applied Thermal Engineering. 2009 Jun 1;29(8-9):1523-31.
[10] Riffat SB, Gan G, Smith S. Computational fluid dynamics applied to ejector heat pumps. Applied thermal engineering. 1996 Apr 1;16(4):291-7.
[11] Varga S, Oliveira AC, Diaconu B. Influence of geometrical factors on steam ejector performance–a numerical assessment. International journal of refrigeration. 2009 Nov 1;32(7):1694-701.
[12] Zhu Y, Cai W, Wen C, Li Y. Numerical investigation of geometry parameters for design of high performance ejectors. Applied Thermal Engineering. 2009 Apr 1;29(5-6):898-905.
[13] Chen W, Chong D, Yan J, Liu J. Numerical optimization on the geometrical factors of natural gas ejectors. International Journal of Thermal Sciences. 2011 Aug 1;50(8):1554-61.
[14] Li C, Li Y, Wang L. Configuration dependence and optimization of the entrainment performance for gas–gas and gas–liquid ejectors. Applied Thermal Engineering. 2012 Dec 15;48:237-48.
[15] Chen W, Chong D, Yan J, Liu J. The numerical analysis of the effect of geometrical factors on natural gas ejector performance. Applied Thermal Engineering. 2013 Sep 25;59(1-2):21-9.
[16] Maghsoodi A, Afshari E, Ahmadikia H. Optimization of geometric parameters for design a high-performance ejector in the proton exchange membrane fuel cell system using artificial neural network and genetic algorithm. Applied Thermal Engineering. 2014 Oct 5;71(1):410-8.
[17] Chong D, Hu M, Chen W, Wang J, Liu J, Yan J. Experimental and numerical analysis of supersonic air ejector. Applied Energy. 2014 Oct 1;130:679-84.
[18] Yang X, Long X, Yao X. Numerical investigation on the mixing process in a steam ejector with different nozzle structures. International journal of thermal sciences. 2012 Jun 1;56:95-106.
[19] Hui X, Ma Y, Deng X. Numerical simulation on effects of augmentation in temperature of inlet steam on wet steam flow in supersonic nozzle: energy and exergy analysis. Multiscale and Multidisciplinary Modeling, Experiments and Design. 2023 Jun 23:1-0.
[20] Aliabadi MA, Bahiraei M. Effect of water nano-droplet injection on steam ejector performance based on non-equilibrium spontaneous condensation: A droplet number study. Applied Thermal Engineering. 2021 Feb 5;184:116236.
[21] Zhang G, Wang X, Dykas S, Aliabadi MA. Reduction entropy generation and condensation by NaCl particle injection in wet steam supersonic nozzle. International Journal of Thermal Sciences. 2022 Jan 1;171:107207.
[22] Zhang G, Wang X, Pourranjbar D, Dykas S, Li H, Chen J. The comprehensive analysis of the relationship between the latent heat, entrainment ratio, and ejector performance under different superheating degree conditions considering the non-equilibrium condensation. Applied Thermal Engineering. 2022 Jan 5;200:117701.
[23] Zhang G, Dykas S, Li P, Li H, Wang J. Accurate condensing steam flow modeling in the ejector of the solar-driven refrigeration system. Energy. 2020 Dec 1;212:118690.
[24] Aliabadi MA, Lakzian E, Jahangiri A, Khazaei I. Numerical investigation of effects polydispersed droplets on the erosion rate and condensation loss in the wet steam flow in the turbine blade cascade. Applied Thermal Engineering. 2020 Jan 5;164:114478.
[25] Ariafar K, Buttsworth D, Al-Doori G, Malpress R. Effect of mixing on the performance of wet steam ejectors. Energy. 2015 Dec 15;93:2030-41.
[26] Ariafar K, Buttsworth D, Al-Doori G, Sharifi N. Mixing layer effects on the entrainment ratio in steam ejectors through ideal gas computational simulations. Energy. 2016 Jan 15;95:380-92.
[27] Ariafar K, Buttsworth D, Sharifi N, Malpress R. Ejector primary nozzle steam condensation: Area ratio effects and mixing layer development. Applied thermal engineering. 2014 Oct 5;71(1):519-27.
[28] Aliabadi MA, Lakzian E, Khazaei I, Jahangiri A. A comprehensive investigation of finding the best location for hot steam injection into the wet steam turbine blade cascade. Energy. 2020 Jan 1;190:116397.
[29] Aliabadi MA, Jahangiri A, Khazaee I, Lakzian E. Investigating the effect of water nano-droplets injection into the convergent-divergent nozzle inlet on the wet steam flow using entropy generation analysis. International Journal of Thermal Sciences. 2020 Mar 1;149:106181.
[30] Aliabadi MA, Zhang G, Dykas S, Li H. Control of two-phase heat transfer and condensation loss in turbine blade cascade by injection water droplets. Applied Thermal Engineering. 2021 Mar 5;186:116541.

[31] Dykas S, Wróblewski W. Single-and two-fluid models

for steam condensing flow modeling. International Journal of Multiphase Flow. 2011 Nov 1;37(9):1245-53.
[32] Hosseinizadeh SE, Ghamati E, Jahangiri A, Majidi S, Khazaee I, Aliabadi MA. Reduction of water droplets effects in steam turbine blade using Multi-objective optimization of hot steam injection. International Journal of Thermal Sciences. 2023 May 1;187:108155.
[33] Dolatabadi AM, Pour MS, Rezaee K, Ajarostaghi SS. Applying machine learning for optimization of dehumidification strategy on the modified model for the non-equilibrium condensation in steam turbines. Engineering Analysis with Boundary Elements. 2022 Dec 1;145:13-24.
[34] Dolatabadi AM, Eghbali MJ, Florin-Emilian Ț, Mohamadpour E, Amini R. Performance evaluation of condensing flow behavior considering magneto hydrodynamics field effects. Applied Thermal Engineering. 2023 Jan 25;219:119472.
[35] Li H, Wang X, Huang H, Ning J, Li A, Tu J. Numerical study on the effect of superheat on the steam ejector internal flow and entropy generation for MED-TVC desalination system. Desalination. 2022 Sep 1;537:115874.
[36] Ruangtrakoon N, Thongtip T, Aphornratana S, Sriveerakul T. CFD simulation on the effect of primary nozzle geometries for a steam ejector in refrigeration cycle. International Journal of Thermal Sciences. 2013 Jan 1;63:133-45.
[37] Cai L, He M. A numerical study on the supersonic steam ejector use in steam turbine system. Mathematical Problems in Engineering. 2013 Jan 1;2013.
[38] Ruangtrakoon N, Aphornratana S, Sriveerakul T. Experimental studies of a steam jet refrigeration cycle: effect of the primary nozzle geometries to system performance. Experimental thermal and fluid science. 2011 May 1;35(4):676-83.